

INVESTIGATION OF AA5083 T-LAP JOINT FABRICATED BY FRICTION STIR WELDING

Phan Thanh Nhan^{1,*}, Tran Minh Khang¹, Tran Hung Tra²

¹*HCMC University of Technology and Education, 01 Vo Van Ngan, Linh Chieu, Thu Duc,
Ho Chi Minh city, Vietnam*

²*Nha Trang University, 02 Nguyen Dinh Chieu, Nha Trang, Vietna*

*Email: nhanpt@hcmute.edu.vn

Received: 7 January 2019; Accepted for publication: 13 May 2019

Abstract. Transportation industries are faced to big matters that the scientists focus on, such as energy saving and ecologically sustainable products. Therefore, many innovative solutions are delivered that will support environmental preservation but meet industries' requirements for greater productivity and minimized operational costs. Aluminum alloys have successfully contributed to meet the rising demand for lightweight structures. Recently, notable developments in aluminum welding techniques have resolved many welding related problems, although some problems need to be addressed. In this paper, 5083 aluminum alloy T-lap-joints were successfully fabricated by friction stir welding with various welding regimes. The defects morphology in the T-joints was experimentally observed and analyzed by a high magnification microscope. The role of the grain microstructure and the effects of defects morphology in the mechanical behavior of the T-joint were investigated. In addition, the fracture locations and the fracture surface of the failure specimens were observed and discussed as well. Results indicate that the fracture of T-joints along the stringer is attributed to the bonding line defects, kissing bond defects and the tunnel defects. The result also shows that, in the T-joints of 5083 aluminum alloy, the welding parameters influence significantly on the features and sizes of the defects.

Keywords: T-joint friction stir welding, defects morphology, microstructure, mechanical properties, aluminum alloy 5083.

Classification numbers: 2.9.1, 5.1.4.

1. INTRODUCTION

Aluminum alloys have been one of the primary candidates for material selection in many industries, including the commercial and military aircraft and marine sectors, for more than 80 years, mainly due to their well-known mechanical behavior, design ease, manufacturability and the existence of established inspection techniques [1]. Increasing utilization of aluminum alloys in various industrial sectors is the main driving force in the search for a viable and efficient technology for joining aluminum alloys that does not cause deterioration in the desirable mechanical, chemical and metallurgical performance of the material [2]. Aluminum alloys are classified as materials difficult to weld or welded with fairly low strength by traditional welding

methods. This is one of the major difficulties in making aluminum alloy structures. Friction-stir welding (FSW), invented in 1991 by the United Kingdom Welding Institute, is a solid state welding technique. The friction-stir welding has emerged as a key technology for joining the alloy with high strength, economic efficiency, friendly environment compared to the quality of traditional welding methods, such as Tungsten Inert Gas welding, Metal Inert Gas welding and Laser Welding [3-5]. This is one of the key techniques to weld aluminum alloys [6-9]. However, this welding process is a complex thermal-mechanical interaction of the metal flow, thus several unsolved issues remain and need to be addressed. Study on the morphology of defects and effects of them on weld quality is a matter of concern to scientists around the world in FSW. Along with that trend, this study focused on analyzing and clarifying the forms of defects arising in friction welds of 5083 aluminum alloy T-lap-joints, thereby giving the appropriate welding parameters and welding tools to minimize defects and to improve weld quality.

2. MATERIALS AND EXPERIMENTS

2.1. Materials

The material used for the experiment is 5083 aluminum alloy (denoted as AA5083) plate having dimension 250×160×3 (mm) for wing plate and 250×50×3 (mm) for stringer plate (Figure 1). The chemical composition and mechanical properties of AA5083 aluminum alloy are given in Tables 1 and 2 [10].

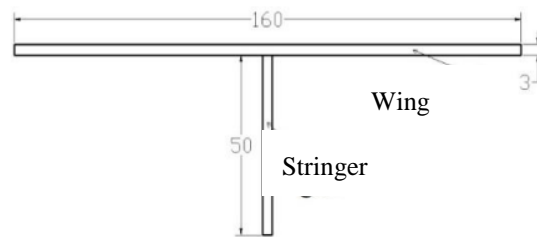


Figure 1. T-lap joint welding.

Table 1. The chemical composition of AA5083 aluminum alloy.

| Element | Al | Mg | Mn | Cu | Si | Zn | Mn | Ti | Cr |
|----------------|---------|---------|-------|---------|---------|----------|---------|----------|-----------|
| Percentage (%) | balance | 4.0-4.9 | 0.4-1 | Max 0.1 | Max 0.4 | Max 0.25 | Max 0.3 | Max 0.15 | 0.05-0.25 |

Table 2. The mechanical properties of AA5083 aluminum alloy.

| Mechanical properties | Yield strength (MPa) | Tensile strength (MPa) | Elongation (%) | Hardness (HRB) | Elastic module (GPa) | Poisson ratio |
|-----------------------|----------------------|------------------------|----------------|----------------|----------------------|---------------|
| Value | 190 | 300 | 16 | 50 | 70.3 | 0.33 |

2.2. Experiments

AA5083 T-lap-joint was fabricated by friction stir welding process, using NTU-FSW machine in Nha Trang University. Welding tool, after designing and manufacturing, was

tempered at 1030 °C and annealed at 600 °C. After heat treatment, hardness of welding pin achieved 47 HRC. Two 5083 aluminum alloy panels are fixed on the table thanks to specially designed jigs. The welding pin is tilted 2 degrees from the plane containing the centerline of tool and the centerline of welding (Figure 2). The main dimensions of welding tool are shown in Table 3.



Figure 2. T-lap joint welding install.

Table 3. The description of welding tool.

| Description | Pin height (mm) | Average diameter of pin (mm) | Shoulder diameter (mm) | Pin shape | Tool material |
|-------------|-----------------|------------------------------|------------------------|-----------|---------------|
| Value | 5 | 5 | 16 | Cone | Steel H13 |

Several T-joints were fabricated by various welding regimes by combining the tool rotation (at 600 rpm) and various welding speeds (from 100 mm/min to 200 mm/min). After welding, we observed the microstructure of the weld after etching with solution 150 ml H₂O, 3 ml HNO₃, 6 ml HF and 6 ml HCl [3] using the Electromet 4. The tensile strength of the weld is performed on the machine Instron 3366 with a speed of 5 mm/min. Specimens are fabricated according to ASTM E8 [11] (Figure 3). The fracture surfaces were observed by the Scanning Electron Microscope (SEM). The weld hardness was measured on Rockwell equipment with HRB scale using ball bearing with 100 kg load.

3. RESULTS AND DISCUSSION

3.1. Microstructure of the weld

3.1.1. The cross-section of the weld

Figure 4 displays the cross-section of the specimens in different welding regimes. The size of defects seems to be proportional to the welding speed. At low welding speed, the joint might be obtained without defects (at 600/100 rev/mm).

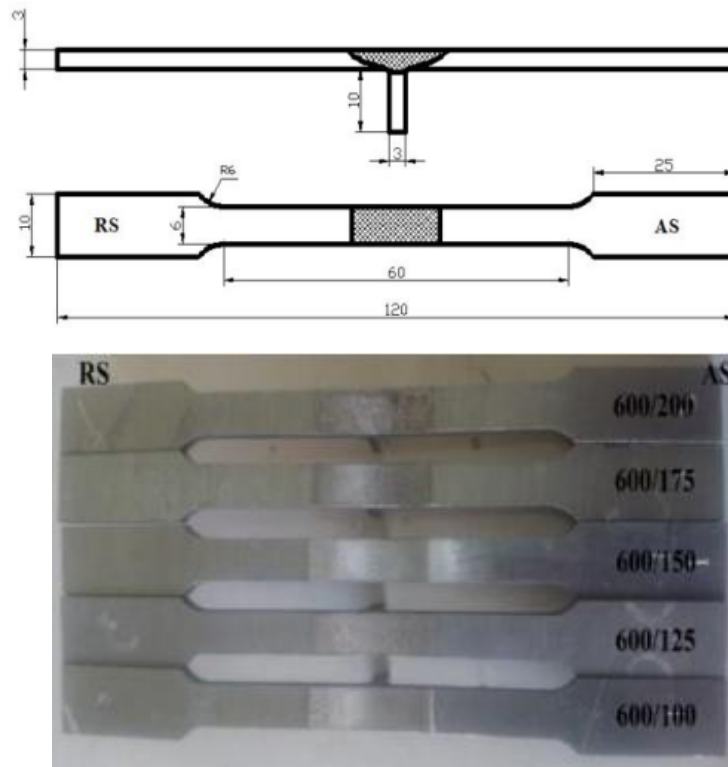


Figure 3. The shape and dimension of specimens.

3.1.2. The grain structure of the weld

Observing the microstructure in the stirring zone (SZ), we see that the grain size ranges from $4 \div 8 \mu\text{m}$ and is much more uniform than the base material (Figure 4). The thermo-mechanically affected zone (TMAZ) has an average grain size of about $15 \div 20 \mu\text{m}$. The heat affected zone (HAZ) has a larger grain size compared to base materials, grain size ranges from $15 \div 45 \mu\text{m}$. The base material (BM) has an irregular grain size of about $10 \div 35 \mu\text{m}$ (Figure 5).

3.2. Investigation of defect types

From Figure 6, tunnel defects always appear at the advancing side (AS) corner of the weld, significantly reducing the cross-sectional area of the welding. Bonding lines tend to move to the SZ, represented by a curve connecting the aluminum oxide that exists inside the weld. The results showed that the kissing bond defects seem to be disappeared in both sides of the wing skin but formed in the AS corner of the T-weld. With the welding regime 600/150 (rev/mm) on the surface appears too many ribbon flash defects that will reduce the amount of material in the welding area. At a high welding speed, regime 600/400 (rev/mm), the cracks on the surface of the weld are unavoidable due to lacking of the filled material.

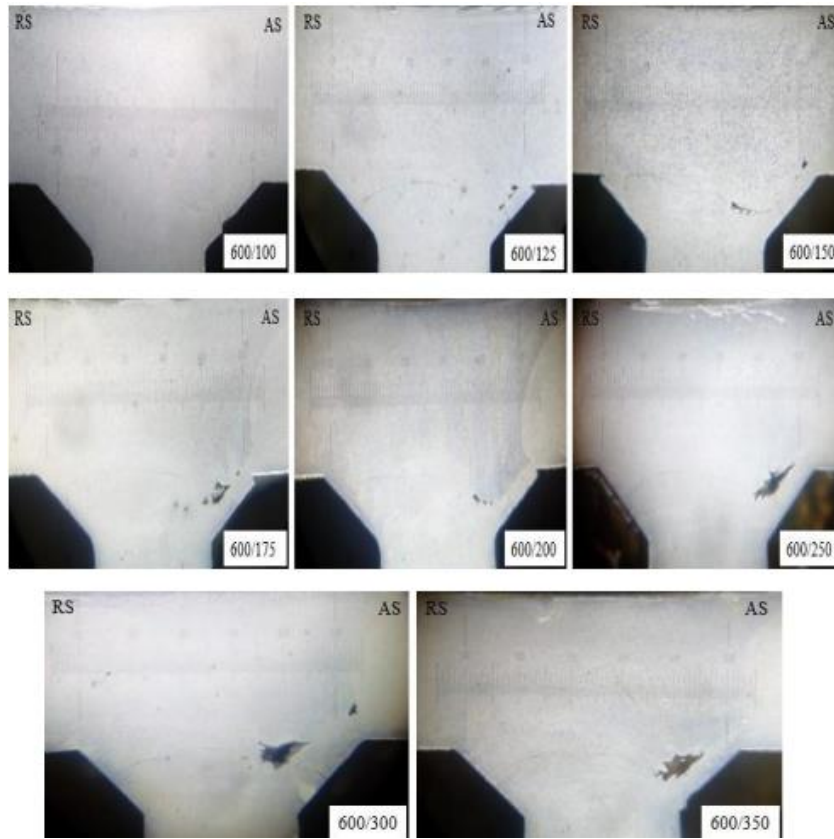


Figure 4. The cross section of specimens at various welding regimes.

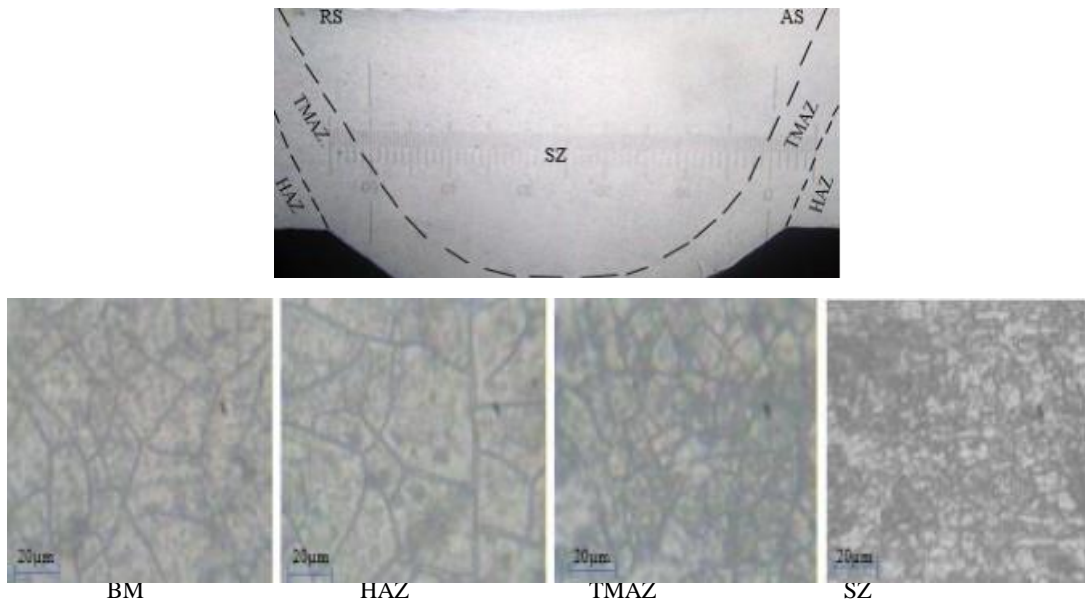


Figure 5. Grain microstructure in welding regime of 600/100 (rev/mm).

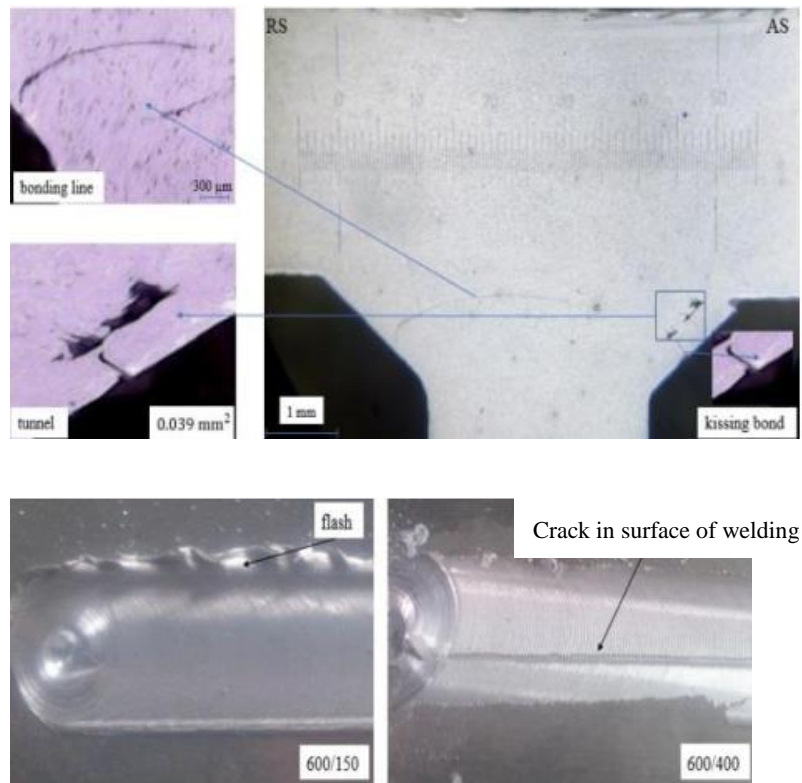


Figure 6. The defect types in welding.

3.3. Influence of welding regimes on the formation of defects

Figures 7 and 8 show that when the transverse speed (v) of the tool increased, the area of tunnel defects and length of bonding line increased significantly and led to the low weld quality.

3.4. Investigation of correlations between defect types with tensile strength

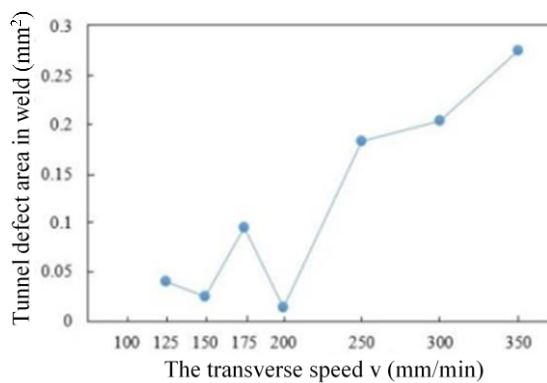


Figure 7. Influence of transverse speed on tunnel defect area in welds.

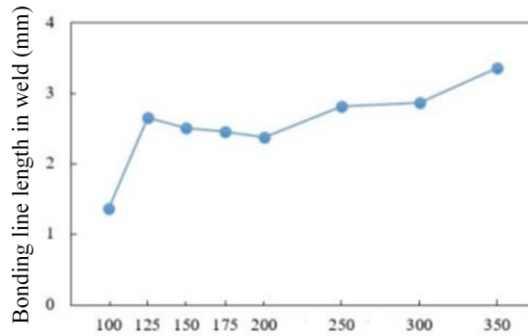


Figure 8. Influence of transverse speed on bonding line length in welds.

Figure 9 shows the effect of transverse speed on tensile strength of wings and stringer in weld. At three regimes of tool transverse speed of 125, 175, 200 mm/min, the strength of wings approximates 86 % compared to the strength of the base material.

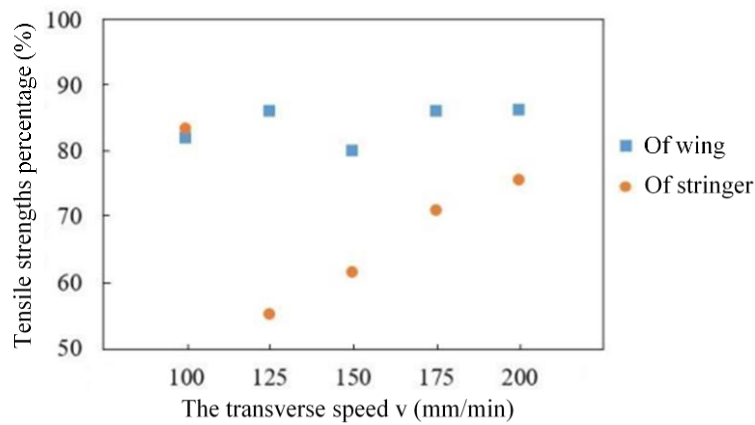


Figure 9. Influence of transverse speed on weld strength.

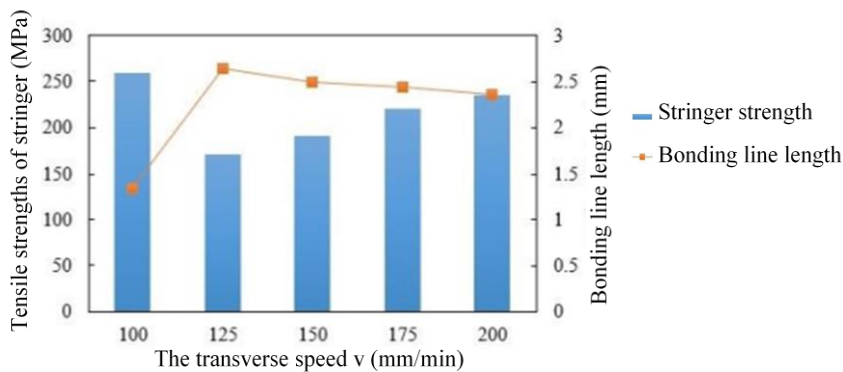


Figure 10. Correlation between stringer strength and bonding line length.

Figure 10 describes correlation between bonding line defect and tensile strength in stringer depending on transverse speed of tool. Here, the bonding line length is inversely proportional to the stringer tensile strength. Because of this, to increase the strength of stringer we need to remove bonding line defects by reducing the transverse speed.

3.5. Destruction position

Table 4. Comparison of destruction position on wings and stringer in tensile experiment.

| Regimes (rev/mm) | Wing tensile experiments | Stringer tensile experiments |
|------------------|---|---|
| 600/100 |  |  |
| 600/125 |  |  |
| 600/150 |  |  |
| 600/175 |  |  |
| 600/200 |  |  |

Table 4 displays a comparison of the destruction positions on wings and stringer in the tensile experiments.

In the wing tensile experiments, most of specimens were fractured in the HAZ. The results showed that the wing tensile properties were not affected by bonding line defects, kissing bond defects and tunnel defects.

In stringer tensile experiments, the crack positions appear along the bonding line defects. Therefore, bonding line defects play an important role in cracking source during the springer tensile test. For the weld specimen at regime 600/100 (rev/mm), the wing is deformed remarkably and the destructible surface is oblique to the vertical.

Figure 11 shows SEM images of fail wing surfaces in various welding regime. On destructive surfaces, large and deep dimples appear. It shows that nucleation and crystallization are not different in welding areas and base materials. This indicates that the main factor affecting the wing tensile properties is not from tunnel defects or bonding line defects but here, the main reason is that the grain size in the HAZ is rougher and larger than the ones in other zones.

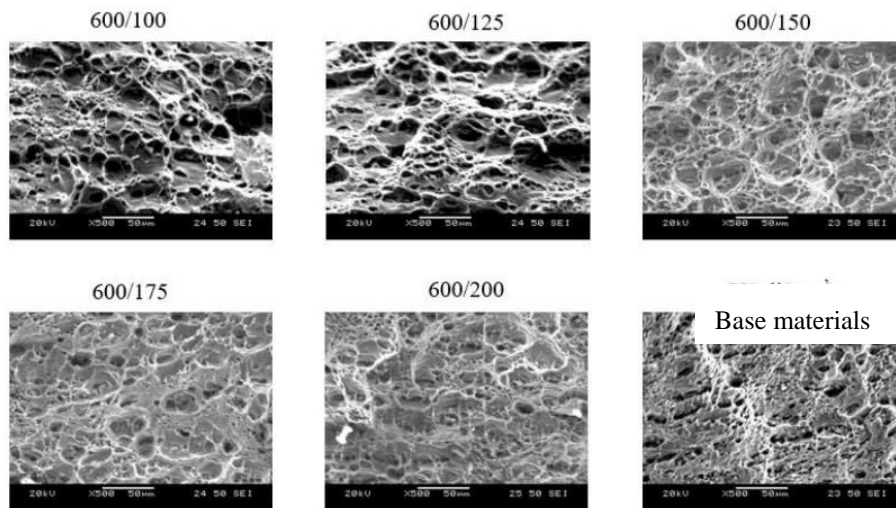


Figure 11. SEM images of fail wing surfaces in various welding regimes.

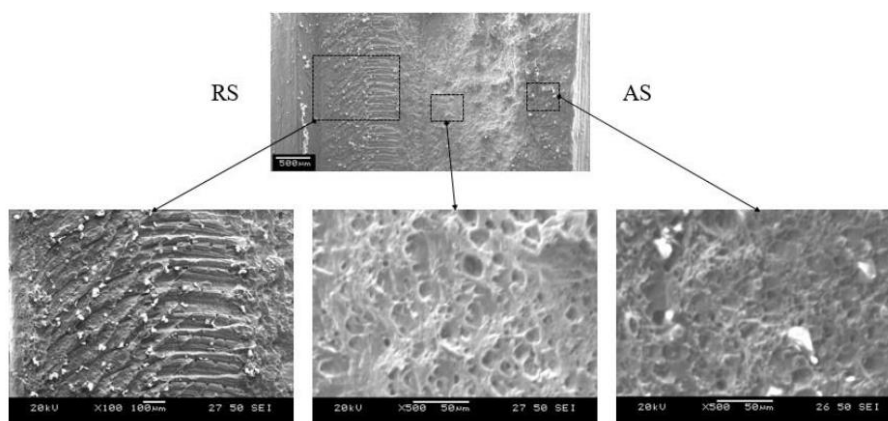


Figure 12. SEM images of stringer fracture surfaces in regime of 600/125 (revolving/mm).

Figure 12 shows SEM images of the stringer fracture surface in welding of 600/125 (rev/mm). We can see that on the AS the weld appear small and shallow dimples, which proves that in this position, the material flow unmixed into each other due to existing kissing bond defects. Observing the central area, the large and deep dimples occupy, showing a dominant plastic deformation characteristic in this area. On retreating side (RS) due to strong metal bonding process, but mixing with aluminum oxide and temperature is not enough to soften metal, therefore the surface is scratched and the material here is quite brittle.

3.5. Micro-hardness of the weld

In five welding regimes, the results show that the position with the smallest micro-hardness is the HAZ (about 5.0 ÷ 15.0 mm from the center of the weld, Figure 13). At the positions 0.0 – 2.0 mm from the center of the weld, the micro-hardness value increased significantly. The results showed that the lowest hardness value was found in the HAZ about 3.9 mm from the surface of the skin (Figure 14).

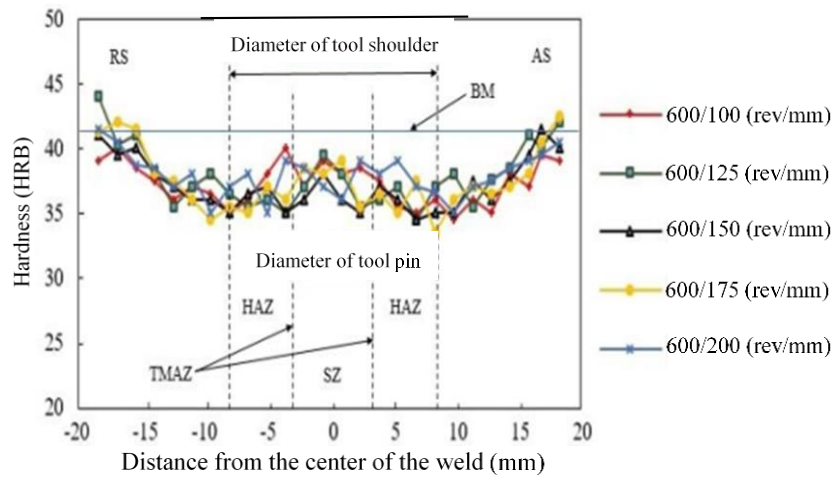


Figure 13. Hardness distribution of welding regimes when measured on the wings

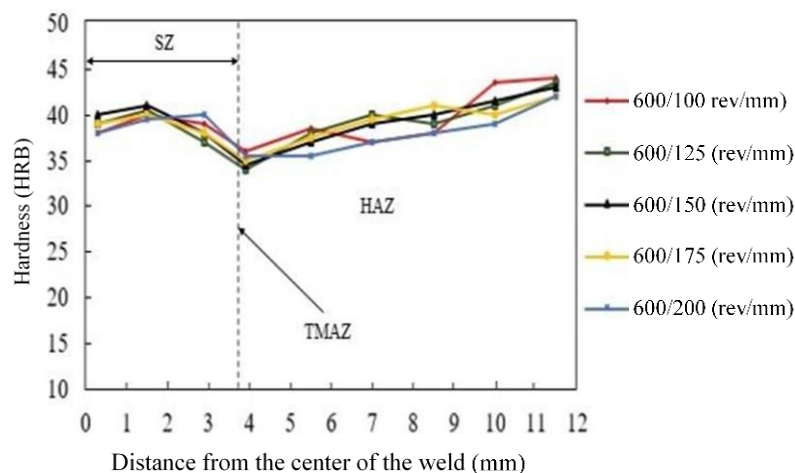


Figure 14. Hardness distribution across the stringers of welds.

4. CONCLUSIONS

In this study, the T-lap friction-stir welding of AA5083 aluminum alloy plates was fabricated successfully. Kissing bond defects, tunnel defects, and bonding line defects are the main factors that affect on the stringer tensile properties of welds. The destruction of specimens when skin tensile testing is due to the formation of grain structure, grain boundaries during recrystallization. The results of this study indicated that, to eliminate bonding line defects and tunnel defects, the transverse speed need to reduce to enhance the weld temperature and material flows.

The study also showed that the weld in regime of 600/100 (rev/min) does not appear the tunnel defects, reaching the skin and stringer tensile strength of 82 % and 83 %, respectively. In this experiment, the HAZ has the lowest hardness when measured along the centerline of the skins. In subsequent studies, we need to focus on studying and investigating cracks, predicting the fatigue life of the weld.

REFERENCES

1. Dursun T., Soutis C. - Recent developments in advanced aircraft aluminum alloys, *Materials and Design* **56** (2013) 862–871.
2. Paul K., Richard R., Jukka M., Raimo S. – Investigation of weld defects in friction-stir welding and fusion welding of aluminum alloys, *International Journal of Mechanical and Materials*, Spring Open Journal (2015) - DOI 10.1186/s40712-015-0053-8.
3. Gene M. - The welding of aluminum and its alloys, Woodhead Publishing Ltd, Cambridge (2002).
4. Ma Z. Y. - Friction Stir Processing Technology: A Review, *Metallurgical and Materials Transactions* **37A** (2008) 642-658.
5. Mishra R.S. - M.W. Mahoney editors, *Friction Stir Welding and Processing*, ASM International (2007).
6. Hao D. D., Okazaki M., Tra T. H., Nam Q. H. - Defects Morphology in the Dissimilar Friction Stir Welded T-lap Joints of AA7075 and AA5083, *Advances in Engineering Research and Application* **63** (2019) 210-216.
7. Hao D. D., Tra T. H. - Effects of friction stir welding parameters on the mechanical properties of AA7075-T6, *Archives of Materials Science and Engineering/ International OCSCO World Press* **77** (2) (2017) 58-64.
8. Tra T. H, Okazaki M., Suzuki K. - Fatigue crack propagation behavior of friction stir welding AA 6063-T5: Residual stress and microstructure effect, *International Journal of Fatigue* **43** (2012) 23-29.
9. Tra T. H. - Effect of weld parameters on the mechanical properties of friction stir welding AA6063-T5, *ASEA N Engineering Journal* **4** (2011) 73-81.
10. ASM Handbook - Properties and Selection: Nonferrous Alloys and Special Purpose Materials, ASM International Handbook Committee, Vol. 2, 1992.
11. ASTM E8/E8M-16a - Standard Test Methods for Tension Testing of Metallic Materials, ASTM International, West Conshohocken, PA, 2016.